Journal of Information Systems Engineering and Management
2025, 10(46s)
e-ISSN: 2468-4376
https://www.jisem-journal.com/

Research Article

F-DL: Fusion of Deep Learning and Image Patch Segmentation for Brain Tumor Detection

Amit Kumar[1*], Rituraj Soni[2], Rakesh Poonia[3]

[1*]Research Scholar, CSE Department, Engineering College, Bikaner (Rajasthan), India.

[2]Assistant Professor, CSE Department, Engineering College, Bikaner (Rajasthan), India.

[3]Assistant Professor, MCA Department, Engineering College, Bikaner (Rajasthan), India.

*Corresponding Author e-mail address:amitpanwar889@gmail.com

ARTICLE INFO

Received: 22 Dec 2024

Revised: 18 Feb 2025

Accepted: 25 Feb 2025

ABSTRACT

The brain's unchecked and fast cell development is what fuels a tumor. It may be deadly if not treated right away. Accurately identifying and classifying it remains difficult despite much effort and encouraging results. It is quite difficult to identify a brain tumor because of the differences in the tumor's location, form, and size. The number of "Brain Tumors (BTs)" is rising quickly worldwide. Deadly brain tumors claim thousands of lives each year. For this reason, proper identification and categorization are crucial to brain tumor therapy. Many methods based on “Deep Learning (DL)” and classical “Machine Learning (ML)” have been developed for BT categorization and detection. It takes a lot of effort to create the hand-crafted features needed by the classic ML classifiers. Conversely, deep learning (DL) has become a popular tool for detection and classification due to its strong feature extraction capabilities. As a result, we presented a model fusion-based convolutional neural network model for brain cancer classification in this research. Enhancement of the model's feature recognition performance was achieved by combining several models, combining deep and shallow features, and adding an attention module. Additionally, several tasks were carried out to improve the model's classification performance, including parameter fine-tuning, data augmentation, and model pre-training. Our fusion model is compatible with ConvNeXt_S and baseline EfficientNet B7 models. The model shows an accuracy of 99.88%.

Keywords: Brain Tumour, Convolutional Neural Network, Deep Learning, Image Classification, Image Segmentation, Machine Learning.

1. Introduction

The most delicate and heaviest organ in the human body is the brain. It oversees nearly all bodily functions. The brain is responsible for controlling various bodily functions, including taste, hearing, vision, sensation, smell, and movement. The brain is the body's central nervous system and control center. It accomplishes this by using an extensive network of connections and neurons to regulate every vital bodily function [1]. One illness that could have potentially fatal effects is a brain tumor. The proliferation of aberrant cells

Journal of Information Systems Engineering and Management
2025, 10(46s)
e-ISSN: 2468-4376
https://www.jisem-journal.com/

Research Article

within the brain is the source of brain malfunction, which also affects the central spine and the nervous system. Its boundaries are well defined, it grows slowly, and it hardly ever goes outside of them [2]. The brain contains billions of active cells, making analysis difficult at times. One of the main causes of death in humans is brain tumors. The “World Health Organization (WHO)” prediction that brain tumors will increase by 5% annually worldwide. Compared to other diseases of the body, brain tumors are more dangerous and challenging to identify. Despite the lack of early therapy each year, 250,000 people worldwide are impacted by brain tumors. The central nervous system of the body with a brain can be affected by 130 distinct types of tumors, which can all vary from very rare to common [3].

A BT is an aberrant brain cell proliferation that occurs inside the brain. Brain tumors can impair brain tissue function and unnecessarily pressurize surrounding areas. BT may potentially result in hemorrhage or interfere with the normal flow of cerebral fluid. As a result, there might be a buildup of fluid and a rise in internal pressure inside the skull [4]. Tumors can arise in any part of the brain and range in size. BTs come in 120 different varieties. The brain's intricate anatomy makes diagnosis and therapy challenging. The BT's origin, size, and location all affect its symptoms. Severe headaches, unexpected seizures, and anomalies in smell, vision, and hearing are the most typical symptoms. Additional signs and symptoms include a change in personality, difficulty falling asleep, problems remembering things, being exhausted all the time, or experiencing nausea and vomiting. Depending on where the tumor is located, symptoms may include visual problems, hearing loss [5], swallowing issues, balance problems, motor skill problems, vision abnormalities, and facial paralysis or weakness [6]. For a thorough diagnosis, it is always advised to speak with a medical expert.

While malignant tumors can take many different forms and include spreading harmful cells, non-cancerous tumors are homogeneous and do not contain any dangerous cells. Active cancer cells can also be found in malignant tumors. Benign tumors may develop slowly, but there is always a potential they could turn into deadly malignant tumors shown in Figure 1. Benign tumors may also be referred to as low-grade tumors. Meningiomas and gliomas are two other subtypes of low-grade tumors, also known as benign tumors [7]. The two kinds of high-grade brain tumors that are classified as malignant tumors, or high-grade brain tumors, are glioblastoma and astrocytoma. Since a benign tumor is not common in other brain regions, it poses no threat. Malignant tumors, on the other hand, grow very quickly and are quite dangerous [8].

Brain tumors can be treated in a variety of ways, and the one selected will depend on the location, size, and type of tumor. Compared to alternative therapies, surgery is currently the most popular and preferred treatment for brain tumors because it does not have any unwanted adverse effects [9]. When diagnosing brain tumors, “Magnetic Resonance Imaging (MRI)” is the most widely used and efficient method. The human soft tissue can be enlarged to provide exact images in all directions, and MRI technology provides information on this structure. An accurate and comprehensive image of the brain can be obtained by neural MRI. An MRI scan is a crucial tool for diagnosing BT. This procedure involves injecting a specific dye to improve the quality of the MRI image and aid in the differentiation of healthy tissues from malignancies [10]. Brain tumors may be present based on the interpretation of the MRI image. The qualities of images obtained from Magnetic Resonance Imaging can vary based on the inside anatomical structures under investigation. The MRI method is highly renowned for its accurate tumor appearance and better image clarity [11]. A large amount of time must be spent, and the radiologist's experience and skill are crucial in making this diagnosis.

Since early diagnosis of tumors is essential to prevent the loss of human life, brain cancers are a prominent issue in the field of neuroscience. Despite the availability of several techniques for detecting anomalies in brain MRI images, there is still potential for advancement and classification in a reasonable amount of time. Early detection is critical for dramatically lowering the fatality rate from brain tumors [12]. Medical imaging has been used extensively by doctors to identify tumors. MRI is a prominent approach to identifying brain

Journal of Information Systems Engineering and Management
2025, 10(46s)
e-ISSN: 2468-4376
https://www.jisem-journal.com/

Research Article

cancers early. Brain tumors are regularly detected manually by radiologists. The radiologist's abilities and knowledge impact how long it takes to grade a tumor. The procedure of recognizing a tumor, on the other hand, is imprecise and costly. Misdiagnosis of a brain tumor can dramatically reduce a patient's chances of survival, resulting in major complications [13]. MRI technology is gaining popularity to solve the limits of human diagnosis. Advancements in “Machine Learning (ML)” and “Artificial Intelligence (AI)” have allowed for early diagnosis of brain cancers. The development of automated image analysis systems has garnered increased attention recently, as a means of circumventing the limitations associated with manual patient diagnosis [14]. A number of computer-assisted diagnosis methods have been developed recently to automatically diagnose brain cancers. Numerous researchers have looked at the classification of brain tumors and have employed a variety of techniques to assess MRI images to extract probable features from the data using DL, and ML. DL is frequently utilized in the medical field for tasks like analysis, classification, and recognition. In 1980, the CNN was first put to use. DL is a state-of-the-art breakthrough in categorization and prediction that has shown exceptional performance in multilayer data processing applications, including speech recognition, identification, and categorization [15].

From images, it is possible to derive underlying tendencies that are valuable and have been shown to boost provincial efficacy. It is the most astounding example of Machine Learning (ML) accomplishment, able to handle difficult object detection utilizing picture datasets and pattern recognition. Due to the need for expertise in classification, manually examining and interpreting such a large volume of data is more time-consuming, expensive, and prone to error [11]. To aid medical practitioners in determining the best course of action and averting brain tumor-related premature death, a DL-based model that accurately and quickly detects brain malignancies will be built. Thus, the primary objective of the research is to offer a useful and organized framework for categorizing brain tumors. The publicly available MRI brain tumor and skin lesion datasets are used to verify the proposed deep learning method. Several performance metrics, including “precision,” “F1-score,” “accuracy,” and “recall,” are employed in this study to assess the results. The main contribution of this work are given below:

1. This work suggests the PC-FT Inception Net model for image partitioning of brain hematomas. To increase the precision of the location, the sections from the unhealthy images are divided into overlapping square patches of the same size. This allows the trained model to focus on identifying certain characteristics inside each patch.
2. This article presented a model fusion-based CNN for the categorization of tumor detection. For the model fusion, ConvNeXt_S and baseline EfficientNet B7 were used as the backbone sub-classification models.
3. To improve the suggested network model's capacity for feature extraction, the Enhanced Channel Focus and Controlled Channel Transformation modules were added to the foundational units of EfficientNet B7 and ConvNeXt_S, respectively. To confirm the correctness of this work, several tests were carried out to compare the suggested model with the standard CNN models that have been in use recently.

The rest of the paper is organized as follows: In the first section, the introduction related to brain disease using MRI image identification is discussed. In the second section, the previous research on brain tumors using various deep learning and machine learning models is discussed. Section 3 presents the proposed model architecture. Section 4 describes the proposed model result. Section 5 provides a final summary of this research as well as potential future opportunities in this field of study.

Journal of Information Systems Engineering and Management
2025, 10(46s)
e-ISSN: 2468-4376
https://www.jisem-journal.com/

Research Article

2. Literature Review

This section discussed the previous work related to the classification and detection of different medical diseases using different deep learning and machine learning models In the fields of healthcare and medical imaging, BT detection is crucial. This topic inspires researchers since early diagnosis is critical to successful therapy and better patient outcomes. Critical illness detection greatly benefits from the application of AI, notably ML and DL-based computer-aided diagnostic (CAD) systems. Compared to medical professionals, the AI-based CAD system analyses brain tumor MRI images more accurately. Still, the predictive accuracy of the AI-based CAD system's visual interpretation is insufficient to reliably identify brain tumors. This section discussed the previous work related to the classification and detection of different medical diseases using different deep learning and machine learning models.

Saeedi S. et al. [16] created a convolutional auto-encoder network and a new 2D CNN, both of which had previously been trained using the hyper-parameters we had been given. Eight convolutional layers, four pooling layers, and batch-normalization layers were implemented after each convolutional layer in this network. Budati A.K. et al. [17] describe an automated model of brain MRI scan tumor categorization and identification using machine learning techniques. The pre-processed images are first segmented using a C-V model to identify the tumor. Key features are then retrieved from the segmented images using GLCM feature extraction, and the images are then classified using SVM and KNN based on the selected derived features. The SVM classifier performs better than the KNN classifier, with an accuracy rate higher than 98%.

Mahmud M.I. et al. [18] examine several models, including ResNet-50, VGG16, and Inception V3, and compare them to the suggested design. They considered many parameters, including accuracy, recall, loss, and “Area under the Curve (AUC)”, to assess the model’s performance. Nassar S.E. et al. [19] help radiologists diagnose brain tumors more accurately, instead of requiring them to examine multiple images, create an effective automated method. The 3064 T1-weighted contrast-enhanced brain MRIs (T1W-CE MRI) from 233 patients serve as the foundation for the suggested methodology. Talukder M. A. et al. [20] have discussed the novel approach that includes thorough pre-processing, rebuilding the architecture for transfer learning, and meticulous tuning. Experiments using 3,064 MRI brain tumor images from Figshare produced precision percentages of 99.40%, 99.68%, 99.36%, and 98.72% for the Xception, ResNet50V2, InceptionResNetV2, and DenseNet201 models, respectively. Our results showed that ResNet50V2 had the greatest accuracy rate, at 99.68%. Zulfiqar F. et al. [21] suggested an approach for improving the pre-existing EfficientNet model.

To identify different types of brain cancers, which included adding many more top layers and a fully linked layer. With EfficientNetB2 serving as the foundation, the suggested approach demonstrated noteworthy performance, achieving an overall test of 98.86% accuracy. A network that improves on the encoder-decoder architecture-based U-Net model by adding skip connections and fine-tuned blocks for feature recognition was created by Yousaf F. et al. [22]. With a specificity of 99.99%, precision of 99.59%, and an F1 score of 99.57%, this model was able to attain an average accuracy of 99.56%. The three forms of brain tumors (BTs) that the researchers classified were "glioblastoma," "meningioma," and "pituitary tumor," among other picture datasets. Raza A. et al.[23] has discussed the "DeepTumorNet," model for combining classic convolutional neural networks (CNNs) with unique deep learning architecture. This design was mostly inspired by the GoogLeNet model; to improve its functionality, the final five layers were eliminated and fifteen new ones were added. To improve the model's performance, the feature map also included a modified version of the leaky ReLU activation function.

The merger of the "Region Proposal Network (RPN)" with the "Faster R-CNN" deep learning technology is suggested by Bhanothu Y. et al [24] for tumor localization and identification. In this technique, the VGG-

Journal of Information Systems Engineering and Management
2025, 10(46s)
e-ISSN: 2468-4376
https://www.jisem-journal.com/

Research Article

16 architecture serves as the basis for both the classifier network and the RPN, providing a strong operational basis. Raza A. et al. [23] A unique deep learning architecture known as "DeepTumorNet" that integrates fundamental CNN structures was introduced by Raza A. and his associates. This design replaces the final five layers of GoogLeNet's core architecture with an extra fifteen, building upon the latter's underlying work. A particular kind of activation function called a leaky ReLU was added to the feature maps to improve the model's performance. In a similar vein, Bhanothu Y. et al. [24] suggested merging the deep learning method known as "Faster R-CNN" with the Region Proposal Network (RPN)" system to locate and classify tumors.

In this technique, the VGG-16 architecture forms the foundation for both the classifier and the RPN. Saba T. et al. [25] proposed a "Transfer Learning" approach called "Visual Geometry Group (VGG-19)" for refining the learned features, which are then combined with manually designed (shape and texture) features in a step-by-step process. The GrabCut technique is employed to precisely delineate the disease symptoms. Entropy is leveraged to enhance these traits for rapid and precise classification, and the classifiers receive a combined vector. Sadad T., and her team [26] showed how to perform segmentation using the U-Net model on the Figshare dataset, utilizing ResNet50 as its core structure, and achieved an intersection over union (IoU) score of 0.9504. Li et al. [27] proposed a method that is contrasted with the hybrid-CNN and hybrid-GAN methods already in use. The results are positive because the accuracy aspect improves and the loss is determined. Asiri A. A. et al. [28] discussed the use of the DL method known as the “Generative Adversarial Network (GAN)”, two neural networks compete to provide artificially realistic data for MRI imaging. The generator and discriminator are the two major components of the GAN network. Our suggested approach is straightforward and 96% accurate. Deepak S. and Ameer P. M. [29] utilized tested models based on different ML models; the fused deep features are categorized. Compared to an advanced method based on CNN trained with cross-entropy loss; the proposed techniques significantly enhance predictions of brain tumors.

2.1. Problem statement

Brain cancers can cause a variety of problems, such as physical disabilities, for which patients must sometimes undergo arduous therapies that are often quite uncomfortable in an attempt to either cure or lessen these consequences. Furthermore, depending on the size, location, and kind of tumor, the effect on brain function might vary. The patient may lose their freedom of movement as a result of the tumor pressing on the part of the brain that controls movement. It may be possible to prevent permanent impairment with early identification. Differentiating the kind of brain tumor presents several difficulties. These difficulties result from the great variability in tumor size, form, and intensity as well as the potential for tumors from other illnesses to have similar outward appearances.

3. Proposed Methodology

The proposed research methodology for fine-grained “Brain Tumour (BT)” classification is outlined and elaborated in this part. There are two primary steps to the proposed technique description. Firstly, described in detail the research dataset that was used to classify BTs at a finer level. Second, went into great detail on the architecture and suggested a deep learning-based method for identifying and categorizing brain MRI pictures into meningiomas, gloom’s, and pituitary tumors. The complete workflows of this work are given in figure 1.

Journal of Information Systems Engineering and Management
2025, 10(46s)
e-ISSN: 2468-4376
https://www.jisem-journal.com/

Research Article

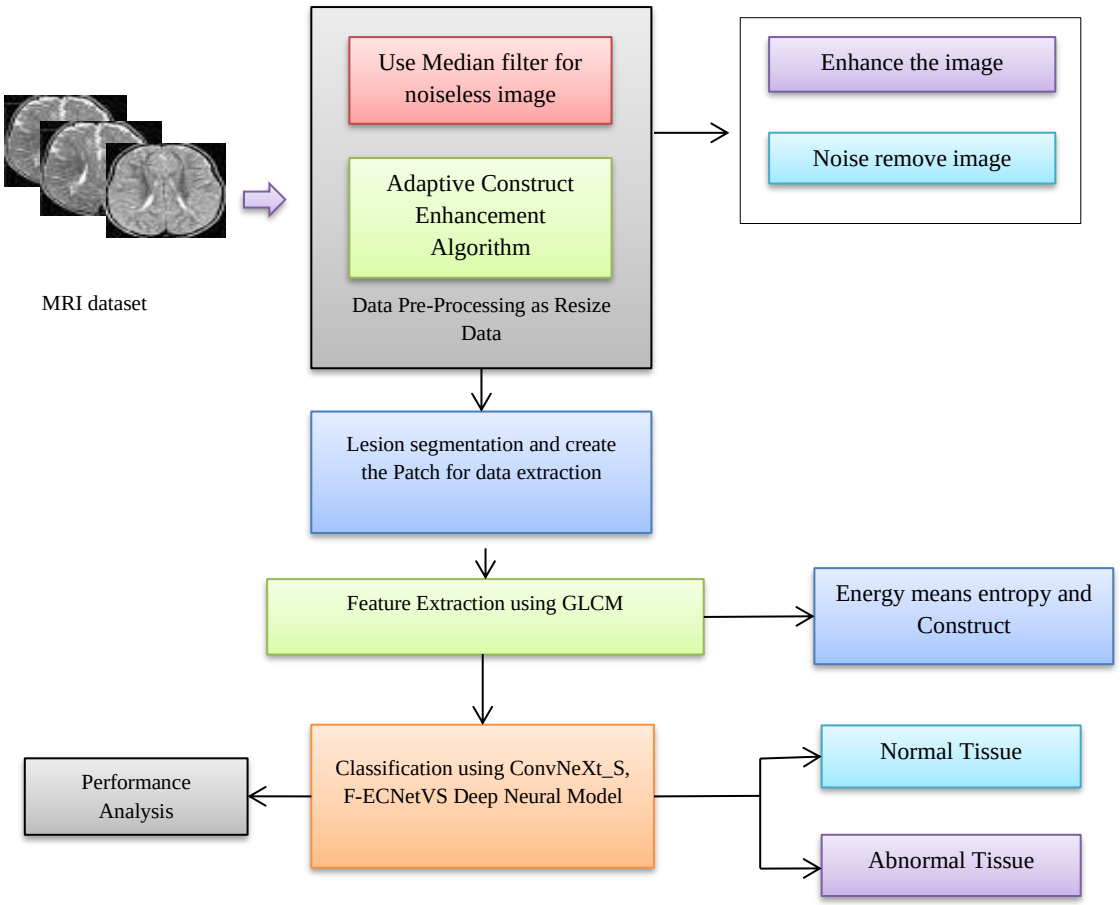

Fig. 1 Workflow of this work

3.1 Dataset: MRI dataset

Data on brain tumors and brain tumor malignancies were gathered from a database that was available to the public [30]. Pictures from "Magnetic Resonance Imaging (MRI)" scans were chosen to create the dataset. Since MRI is thought to be the most reliable approach for diagnosing brain tumors, especially when combined with pictures of lesions associated with brain tumors, we chose to use MRI scans for our investigation. Figure 2 present a summary of the dataset used in the model that was created.

Table 1 Summary of dataset used for the proposedmodel.

Types of Images	Total Count	Training	Testing
Glioma Tumor	926	741	185
Meningioma Tumor	937	450	487
No tumor	500	400	100
Pituitay Tumor	901	721	180

Journal of Information Systems Engineering and Management
2025, 10(46s)
e-ISSN: 2468-4376
https://www.jisem-journal.com/

Research Article

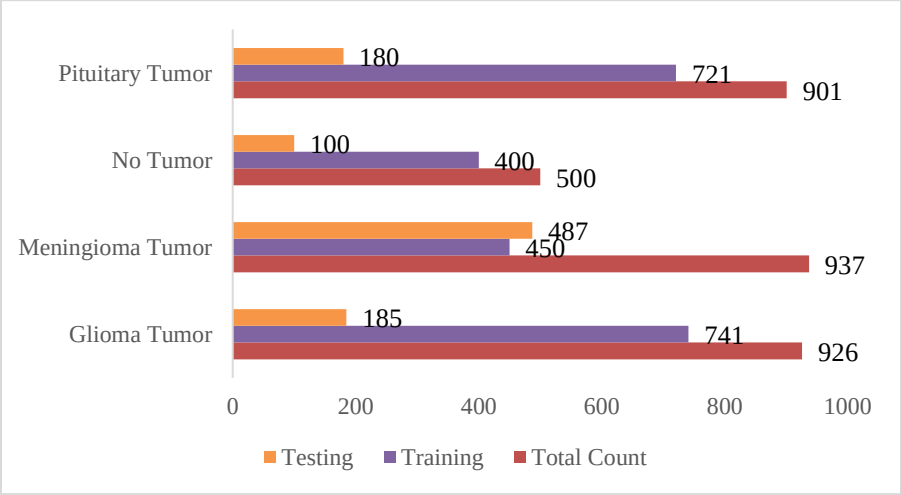

Fig. 2 Summary of the dataset used for the proposed model.

In our dataset, a total of 3264 MRI scans altogether with 2312 images of brain tumor cancer are used for training the model. The MRI images are organized by type of brain tumor in figure 3 and also brain tumor images.

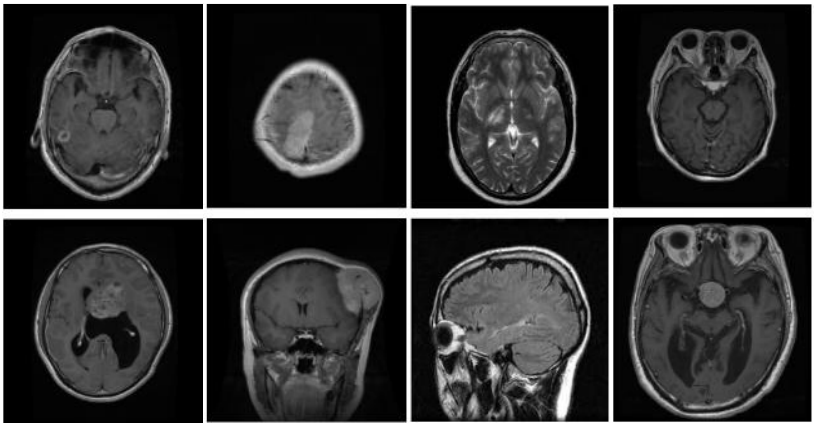

Fig. 3 Sample images of brain tumor.

Fig 3: represents some of the same images of the dataset used in this work. Brain tumor disease is further of three types “Glioma Tumor”, “Meningioma Tumor”, and “Pituitary Tumor” with “No Tumor” type.

3.2 Data pre-processing

The 512×512 resolution dataset photos are sourced from the MRI dataset. The input layer size of 224×224 was used in the creation of the suggested model. As a result, the dataset underwent pre-processing to prepare it for the suggested methodology. The MRI pictures were first downsized and normalized, or transformed to.jpg format. Based on the picture input sizes used by other pre-trained models and our suggested deep-learning model. In this, the division of the dataset is done in the ratio of 80 to 20.

Journal of Information Systems Engineering and Management
2025, 10(46s)
e-ISSN: 2468-4376
https://www.jisem-journal.com/

Research Article

For balancing all the dataset images in this to reduce the overfitting problem we used the data augmentation technique. To improve the model's performance in classification, decrease overfitting, and increase the model's stability during the learning process, we employed data augmentation [31]. Through left-to-right and up-to-down flipping, brightness enhancement, center cropping, application of Cutout, Cutmix, Augmix, and Random Erasing, and the ability to enlarge the training data eight times. The test results, however, won't alter.

3.2.1. Adaptive Contrast Enhancement Algorithm for MRI image

The MRI image contrast plays a crucial role in tumor detection since this method is highly dependent on picture brightness. High-contrast and low-contrast histograms are the two most typical forms seen in MRIs. A technique known as piecewise linear histogram modification is commonly used to improve the contrast of the photos. However, it's difficult to find defined minimum and maximum values that work for every image because the adjustment slope varies across different datasets. Here, we use a flexible and automated way to extract the required characteristics from each picture [32]. A head MRI scan may display blood vessels (V), healthy brain tissue (B), and a brain tumor (T). Initially, we choose a subset of the training set and assign voxels at random to represent the three classes. Next, we forecast each class's intensity probability distribution function (PDF).

A preprocessing method called normalization is applied to the image to align the pixel intensities within a certain range. Normalization is a process that changes the range of pixel intensity values. When working with images from various sources or settings where brightness, contrast, or exposure can vary greatly, this is especially helpful. Normalizing these pixel intensities during convolutional neural network (CNN) training may result in a more stable learning process is shown in equation 1 [30]. Eventually, a multimodal biometric identification system is stronger [33]. Typically, an image's pixel intensities fall between 0 and 255 (for an 8-bit image). These values are rescaled to a new range, typically [0, 1] or [-1, 1], during the normalization process. The following straightforward linear transformation can be used to accomplish this rescaling: The normalized image $S_k(D)_{dig}$ with pixel intensity values q' can be computed as follows given an image $S_k(D)_{dig}$ and pixel intensity values q':

$$q' = \left(\frac{(z-(z_{min})}{(z_{max})-(z_{min})}\right) \quad (1)$$

Where (z_{min}) and (z_{max}) are the minimum and maximum pixel intensity values in the image$S_k(D)$, respectively. This transformation ensures that all pixel intensities in the normalized image $S_k(D)_{dig}$ lie between 0 and 1. This normalization operation is applied to all images in the MRI dataset, yielding a set of normalized images which are then used for feature extraction using CNNs [19], [20]. The advantages of normalization include but are not limited to: (i) it brings consistency in the dynamic range of pixel intensities (ii) it helps in mitigating the effects of lighting variations, which can be quite beneficial for feature extraction from MRI dataset images; (iii) normalized images often lead to a more stable and faster convergence during the training of neural networks [21], [22]. In the Algorithm 2, (z_{min}) and (z_{max}) represent the CLAHE process in the images $S_k(D)_{dig}$, respectively. The normalization operation transforms the original intensity value of a pixel p to a normalized value q' that falls in the range [0, 1]. The whole procedure is carried out for every imagein the set q', resulting in a set of normalized images q'. Next, the CLAHE process involves two steps the first step is the generation of non-overlapped tiles in the image. The image is separated into what are called tiles small, non-overlapping areas. These tiles are usually 8 by 8 pixels in size. Another is the hologram of pixel intensity. The histogram of the pixel

Journal of Information Systems Engineering and Management
2025, 10(46s)
e-ISSN: 2468-4376
https://www.jisem-journal.com/

Research Article

intensities in each tile is calculated, and histogram equalization is implemented. This entails translating the tile's pixel intensities according to a cumulative distribution function (PDF) that is computed from the histogram [34]. Algorithm 1 describes how to normalize the picture using Contrast Limited Adaptive Histogram Equalization (CLAHE).

Algorithm 1: Normalization of the image using Adaptive contrast enhancement

---

Inputs: Dataset $\boldsymbol{S_k(D)_{dig}}$, $\boldsymbol{s \times s}$ as tile size, $\boldsymbol{CL}$ as contrast limit
Outputs: Set of enhanced images $\boldsymbol{S_k(D)_{ct}}$

---

1. Take $S_k(D)_{dig}$ dataset and set $s \times s$ pixel tile
2. Divide $S_k(D)_{dig}$ into non-overlapping tiles set $S = \{s_1, s_2, s_3, \ldots \ldots \ldots \ldots s_n\}$.
3. For each tile S in $S_k(D)_{dig}$
4. Compute the histogram as $H_i = card\{u, v | i(u, v)| = i\}$ H of pixel intensities in $S_k(D)$. Where $card$ set of the size of the pixel such that $i(u, v) \epsilon [0, k-1]$ and $K = 2^8 = 256$ and u, v pixel value.
5. Clip the histogram H at the contrast limit CL to obtain the clipped histogram H_i.
6. Compute the Cumulative Distribution Function (CDF) for H' as $CDF(x) = \sum_{i=0}^{n} p(u')\ \forall\, u' \leq u$ where $(u') = \frac{p(u')}{s \times s}$ and $s \times s$ pixel intensities for $s \times s$ as $u' = CDF(u)$
7. Append $S_k(D)_{dig}$ to the set $S_k(D)_{ct}$.
8. Return→ $S_k(D)_{ct}$

For the $\boldsymbol{S_k(D)_{dig}}$ dataset and the given $\boldsymbol{s \times s}$ pixel tile, the picture has been normalized using contrast-limited Adaptive Histogram Equalization (CLAHE) to improve its contrast. The Division of $\boldsymbol{S_k(D)_{dig}}$ into non-overlapping tiles and find the set $\boldsymbol{S}$. Furthermore, each tile $\boldsymbol{S}$ in has set in $\boldsymbol{S_k(D)_{dig}}$ and compute the histogram as $\boldsymbol{H_i = card\{u, v | i(u, v)| = i\}}$ H of pixel intensities in $\boldsymbol{S_k(D)}$. The Clip the histogram H at the contrast limit CL to obtain the clipped histogram $\boldsymbol{H_i}$ and compute the Cumulative Distribution Function (CDF) for H' append $\boldsymbol{S_k(D)_{dig}}$ to the set $\boldsymbol{S_k(D)_{ct}}$. There is few samples are given in Figure 5 which has generated after applying the CLAHE algorithm in the dataset.

3.3 Lesion semantic segmentation and Patch extraction

The process of splitting a picture entails altering and improving the understandability of its depiction. This procedure finds similar pixels to form a cluster. Here, tumor segmentation is accomplished through the use of an unsupervised technique. The tumor images are first filtered to eliminate noise and undesired background images, and then lesion regions are extracted using Semantic segmentation. Automatic initialization of seed points is used in a region-growing approach for segmentation. Figure 4 shows the detected lesion from the MRI image.

Journal of Information Systems Engineering and Management
2025, 10(46s)
e-ISSN: 2468-4376
https://www.jisem-journal.com/

Research Article

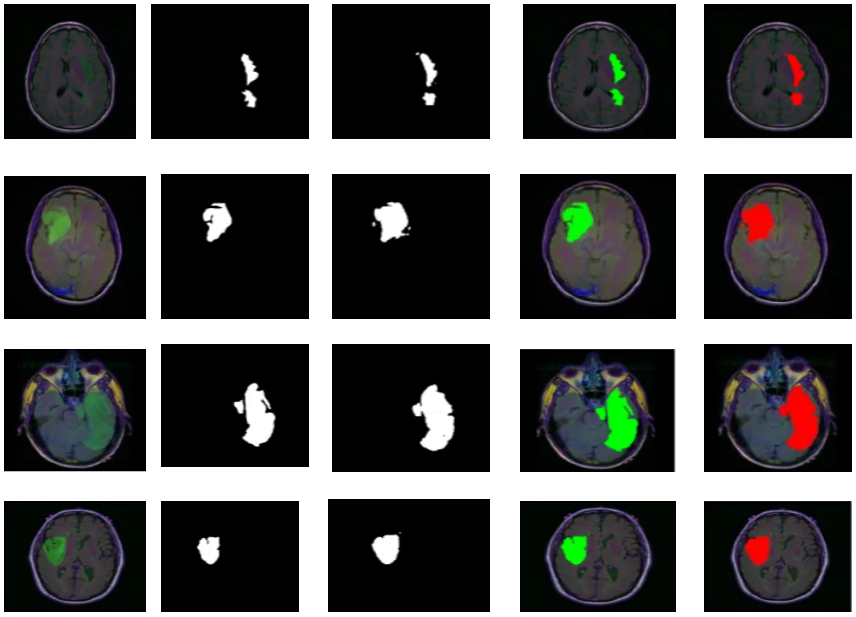

Fig. 4: Lesion object detection using semantic segmentation a. Enhanced MRI image b. Remove background for object c. Remove background for lesion discrimination d. Remove background for lesion discrimination and e. Segmented tumour

Several widely recognized metrics are used to quantify the segmentation performance, and the outcomes are noteworthy. Then, color and texture characteristics are used to depict the extracted lesion regions. Instead, in patch-based classification, individual picture patches are assigned to a particular class, and the full image is then classed according to the patch classifications[29].

3.3.1 Overlapped Patch Generation

As seen in Figure 5, the original lesion pictures are divided into smaller, overlapping squares, each measuring $q \times q$ pixels. These overlapping segments are formed by selecting a stride of pixels. A 32×32 square section has 1024 pixels in total. A segment is categorized as a vertebra or foreground patch if the total number of pixels in it is 515 or more; otherwise, it is categorized as a background segment [35]. For the training dataset in this work, overlapping segments were produced using a certain stride.

Journal of Information Systems Engineering and Management
2025, 10(46s)
e-ISSN: 2468-4376
https://www.jisem-journal.com/

Research Article

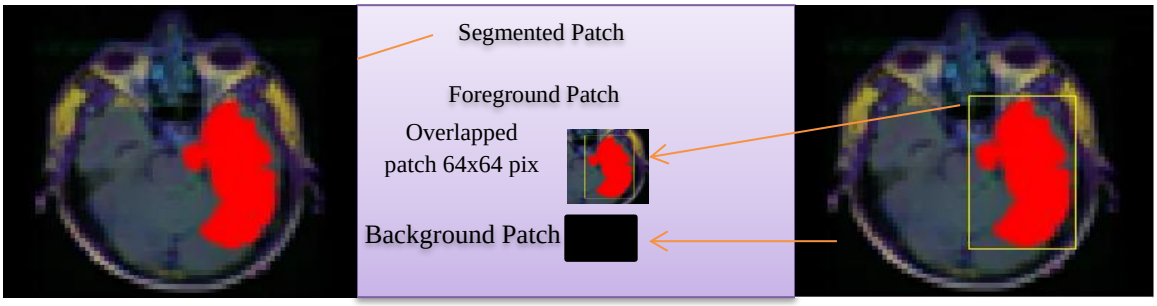

Fig. 5 Overlapped patches of size 64x64 pixels (per frame)

To verify the correctness of the model, testing pictures are further split to create $p \times p$ pixel size overlapping patches. The vertebrae are then segmented from images from the MRI dataset. The next section discusses patch extraction.

3.3.2. Patch Generation of segmented object

To reduce the amount of computing work needed to train the model, the extraction of patches is a crucial step in the segmentation of brain tumor disorders. This is because it allows the deep learning algorithm to take in information from certain areas of the picture. Patches from the pre-processed MRI dataset were collected for use in the convolutional neural network in this study. The Simple TensorFlow framework, which provides a Python-based interface for analyzing medical images, was used to extract the patches. These patches were often recorded as separate picture files or as NumPy arrays, which were then used in the training stage of the deep learning model [36]. The dataset's year, the size of the patch used for extraction, the stride size used to move the patch window across the picture, and the total number of patches extracted from each image are all listed in Table 2. For every picture, the patch and stride have the following dimensions: 32×32, 64×64, and $128 \times 128 \times 3$. The amount of patches that were extracted ranged from 224 to 289 depending on the picture. Furthrmore, datasets with image ID, patch size, stride, and patch count are givn in table 2.

Table 2 Datasets with image ID, patch size, stride, and patch count.

Layer	Filter Size	Stride	Filters	Input Data	Output Data
Conv1	3 × 3	1	32	MRI Images	Feature Maps
Conv2	3 × 3	1	64	Feature Maps	Feature Maps
Conv3	3 × 3	1	128	Feature Maps	Feature Maps
Conv4	3 × 3	1	256	Feature Maps	Feature Maps
Conv5	3 × 3	1	512	Feature Maps	Feature Maps
Conv6	3 × 3	1	1024	Feature Maps	Feature Maps
Conv7	1 × 1	1	2048	Feature Maps	Softmax Output

Journal of Information Systems Engineering and Management
2025, 10(46s)
e-ISSN: 2468-4376
https://www.jisem-journal.com/

Research Article

The process of breaking up the pre-processed illness pictures into smaller areas, or patches, is known as patch extraction. This stage lowers the computational cost of training the deep learning model and enables it to pick up knowledge from localized, tiny characteristics in the photos. Each patch is usually a fixed-size sub-image of the brain tumor portion, such as 64 × 64 or 128 x 128 pixels that are tiny, square, or rectangular. The tumor's size and the computing resources at hand are taken into consideration while selecting the patch size. Larger patches tend to capture more global brain tumor properties, whereas smaller patches tend to catch more localized aspects. The patches are extracted using a sliding window technique, which implies that neighboring patches overlap somewhat, to guarantee that the entire disease is covered. Every pixel in the brain tumor disease is covered by at least two patches since the overlap is typically half the patch size [37]. The few samples of patches, which have been randomly selected from the MRI dataset with pixel size 64 × 64 pixels are given in figure 6.

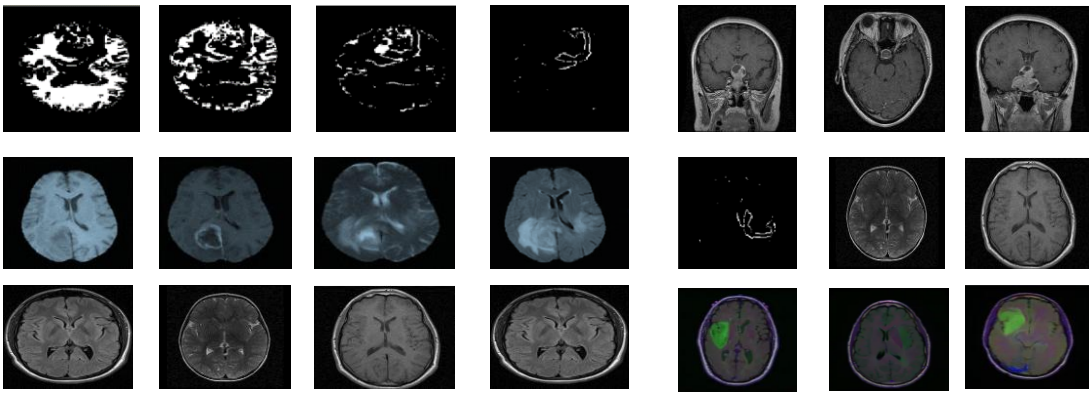

Fig. 6 Sample of patches, which have been randomly taken

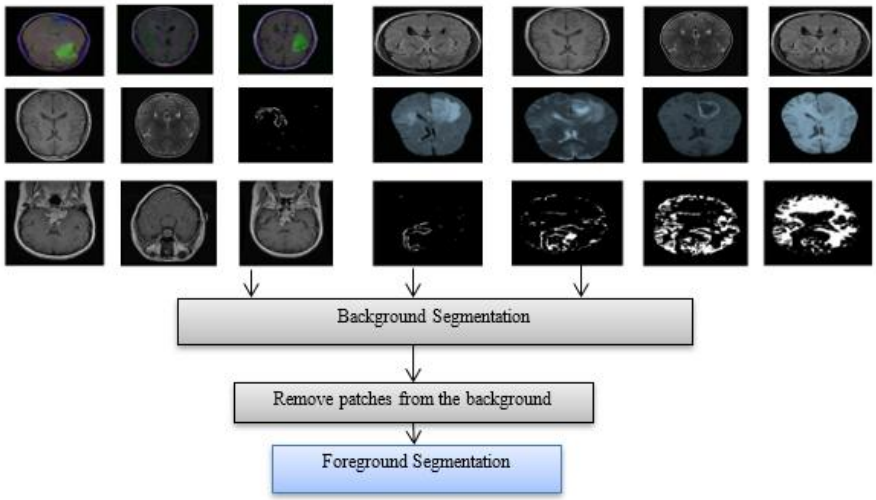

Fig.7 Implement a Random under-sampling method for class imbalance and remove patches from the background

Journal of Information Systems Engineering and Management
2025, 10(46s)
e-ISSN: 2468-4376
https://www.jisem-journal.com/

Research Article

3.4 Remove Background Patches Using Random Sampling Method

Figure 7 class distribution illustrates the unequal distribution of training patches across the two classes we utilized for classification. Since the space of the vertebra in the photos is much smaller than the surrounding region, and the majority of the training instances are tagged as 0, this suggests that the classifier may be biased toward the background. For medical purposes, a high success rate in vertebra patch identification is essential; yet, in real-world scenarios, the rate of incorrectly categorizing vertebra patches as background is unsatisfactory. An equal proportion of both positive and negative examples in the training data is required to overcome this problem [38]. Figure 7 shows how the Random Sampling method is used for class imbalance and removes patches from a background from MRI image patches to eliminate the majority of class patches (background patches). For negative samples, we utilized the random under-sampling method and produced a balanced training set to address this issue. Consequently, during the training phase, this raises the network's accuracy and convergence rate. To create balanced classes before the training step. In next section has covered the proposed model for patch data classification using the EfficientNet B7, ConvNeXt_S, and F-ECNetVS Model.

3.4.1 Feature extraction using Gray Level Co-occurrence Matrix (GLCM).

Tumor classification relies heavily on the process of gathering and selecting pertinent information (Jafarpour et al. 2012). The categorization procedure then makes use of these properties. In this phase, choosing the best characteristics is a challenging challenge. In this procedure, the picture features are identified using the GLCM method. The second-order statistical texture of a given brain picture is found using a statistical technique known as the co-occurrence matrix. The number of gray levels in the GLCM technique must correspond to the rows and columns of the matrix. The characteristics based on the first level of the histogram are obtained using the following formulae.

$$Entp = \sum_{x=0}^{mk-1} \sum_{y=0}^{mk-1} T_{xy} log\ T_{xy} \quad (2)$$

A random variable's entropy may be thought of as a measure of its degree of uncertainty shown in equation 2. The co-occurrence matrix's entropy will increase to its maximum if all of its elements are identical.

$$Correletion = \frac{\sum_{x=0}^{mk-1} \sum_{y=0}^{mk-1} (x,y)t(x,y) - \mu_i \mu_j}{\sigma_i \sigma_j} \quad (3)$$

The similarity between the reference pixel and its neighboring pixels is gauged by the linkage indicator is given in equation 3.

$$Energy = \sum_{x=0}^{mk-1} \sum_{y=0}^{mk-1} T_{xy}^2 \quad (4)$$

The unit of measurement used to get the total squared components is energy is shown in equation 4. This shows how consistent the mix is. Pixels with a high degree of similarity will have a higher energy value.

$$Constrast = \sum_{m=0}^{mk-1} m^2 \sum_{x=0}^{mk-1} \sum_{y=0}^{mk-1} T(x,y)^2 \quad (5)$$

Contrast in a picture is the variation in brightness between a pixel and its neighbor is shown in equation 5. The feature extraction of data are given in figure 8.

Journal of Information Systems Engineering and Management
2025, 10(46s)
e-ISSN: 2468-4376
https://www.jisem-journal.com/

Research Article

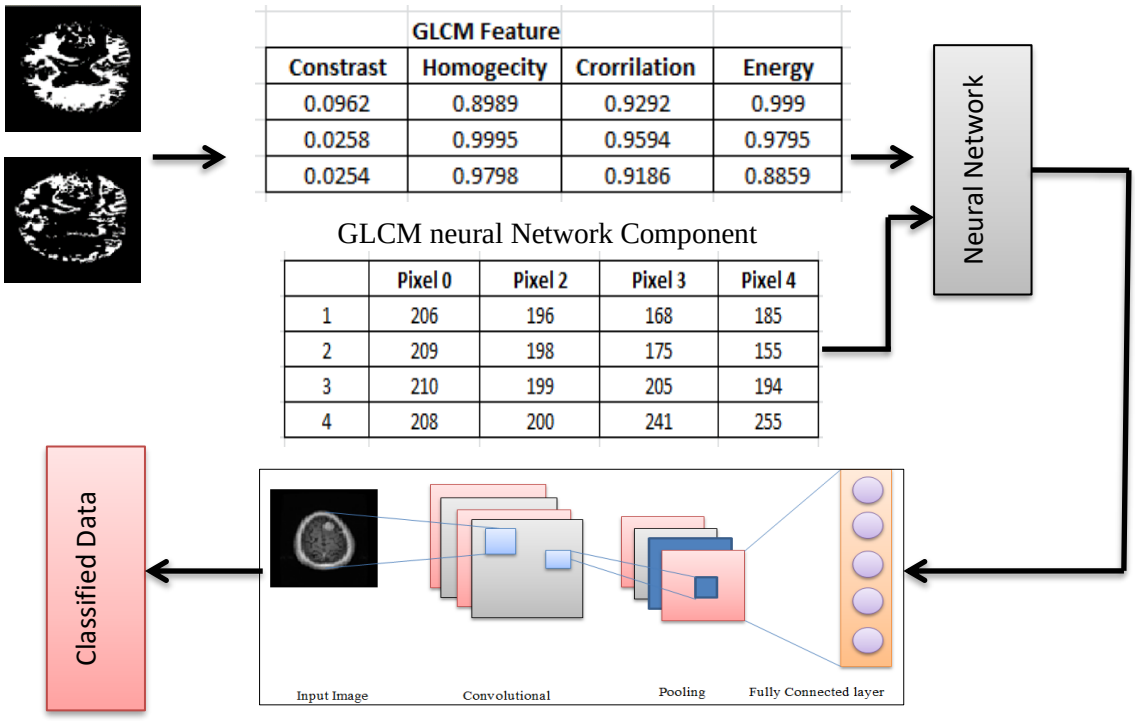

Fig. 8 GLCM-CNN feature extraction

3.5 Classification using Improved Efficient Net B7 model

After the first round of data cleaning, the second stage employs the transfer learning strategy in conjunction with the Convolutional Neural Network (CNN) technology to classify the images of illnesses that impact tomato plant leaves. A simple multiple-layer convolutional neural network architecture is shown in Figure 9. The convolutional layer, which is the first layer, is essential for recognizing the texture of the leaf since it extracts its characteristics. A pooling layer then processes these data. The resolution of the image is decreased without sacrificing quality thanks to this pooling layer. Decisions are made by the completely linked final layer using the characteristics that were taken from the earlier layers. Transfer learning is used in this study to improve the accuracy of the model. To enhance the model's performance, this method makes use of pre-existing artificial intelligence models that have been trained on a variety of datasets [39]. EfficientNet B7 is one method that might be used; it has 740 layers that are intended to improve the accuracy of diagnosing different types of tomato leaf diseases.

Journal of Information Systems Engineering and Management
2025, 10(46s)
e-ISSN: 2468-4376
https://www.jisem-journal.com/

Research Article

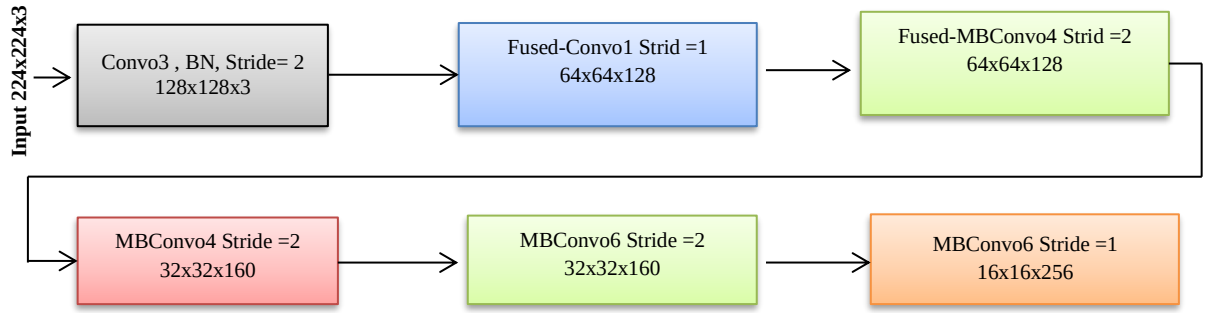

Fig. 9. Architecture of EfficientNet B7

An extra layer is added at the beginning of the fine-tuning phase, consisting of a completely linked layer customized for the quantity of illness labels. The model's top layer is then configured to stay that way, prohibiting any changes or retraining. Figure 9 depicts EfficientNet B7's whole structure.

A group of models known as EfficientNet B7 was created with FLOPs (floating-point operations) and efficient parameter usage in mind. To determine which initial EfficientNet B7 model provides the optimum trade-off between accuracy and FLOPs, it employs NAS (Neural Architecture Search). Then, using an approach that mixes scaling, this initial model is enlarged to provide a spectrum of models, from B1 to B7 [39]. These models frequently perform worse than EfficientNet B7 in terms of parameter and FLOPs efficiency, despite several recent research reporting notable gains in both training and inference durations (as seen in Table 3). The objective of this study is to optimize the training procedure while maintaining parameter efficiency.

Table 3. EfficientNet B7 has good parameters and FLOPs efficiency.

Name of Model	Top-1 Acc.	Params	FLOPs
EfficientNet B7	98.45.60%	43M	19B
ConvNeXt_S	84.40%	192M	64B
F-ECNetVS	99.70%	133M	36B

3.5.1 Improved ConvNeXt_S model

This work has used the ConvNeXt_S model. The transformer architecture, which was originally designed for problems in natural language processing, was enhanced with the creation of the ConvNeXt model [23]. The encoder and decoder modules that comprise the transformer structure are taught to handle data sequentially. By including convolutional layers into the encoder and decoder modules, ConvNeXt expands on the transformer structure and makes it capable of extracting information unique to each images. With this feature, ConvNeXt may take use of the attention mechanism of the transformer while concentrating on certain areas of a picture. ConvNeXt uses a parallel convolutional architecture, which increases the model's capacity and improves its performance in image recognition tasks, in contrast to traditional convolutional neural networks, which typically comprise a series of convolutional layers followed by fully connected layers

Journal of Information Systems Engineering and Management
2025, 10(46s)
e-ISSN: 2468-4376
https://www.jisem-journal.com/

Research Article

[24]. Compared to conventional transformer models, ConvNeXt models provide some advantages for image identification tasks [30]. Figure 10 shows the architecture of ConvoNetXt_S.

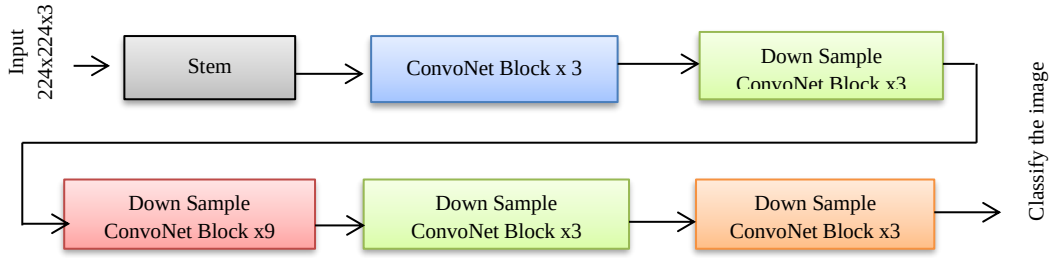

Fig. 10 Architecture of ConvoNetXt_S

This work has used ConvoNetXt_S model for image classification and this process has involved four steps. First is spatial information. The layout data includes transformers that were originally designed for applications such as natural language processing, where word arrangement matters more than precise position. Nevertheless, the way the pixels are arranged in a picture is crucial for tasks involving image identification. Such layout details may be captured by the convolutional layers of the Convolutional Network Xt (ConvoNetXt_S), which enables the model to identify local properties in the picture. The effectiveness of the parameters is the second factor. Because attention matrices are used so frequently in transformers, their efficiency is low and this might limit their scalability.
ConvoNetXt_S uses a two-layered convolutional architecture that maximizes the model's capacity while reducing the amount of parameters it uses, increasing its processing power and memory efficiency. Its resistance to changes in object size is its third benefit. When it comes to controlling object sizes, ConvoNetXt_S outperforms conventional transformer models. ConvNeXt models use convolutional layers that can change their receptive field sizes, enabling them to extract features at different scales, in contrast to transformer-based models that have a fixed receptive field that never changes. ConvoNetXt_S also boasts better accuracy performance [40]. Compared to transformer-based models and EfficientNet B7 networks, they have outperformed them on many image recognition benchmarks, including ImageNet. In conclusion, ConvoNetXt_S's use of convolutional layers provides a more effective and efficient method of using transformers' skills for image recognition applications.

3.6 Fusion or Macro design of EfficientNet B7 and ConvoNetXt_S models

Figure 11 shows the fundamental architectural architecture of the proposed ConvoNetXt_S and EfficientNet B7 models (F-ECNetVS). A fusion method forms the foundation of the model. Two network branches—one for processing RGB data and the other for depth data are used in this fusion. They are taken from the ConvNext model [7]. The F-ECNetVS architecture and extra layers added for multi-scale improvement served as inspiration for the fusion process, which was modeled after the ESANet [15]. Figure 11 shows the topology of the data flow in the F-ECNetVS model.

Journal of Information Systems Engineering and Management
2025, 10(46s)
e-ISSN: 2468-4376
https://www.jisem-journal.com/

Research Article

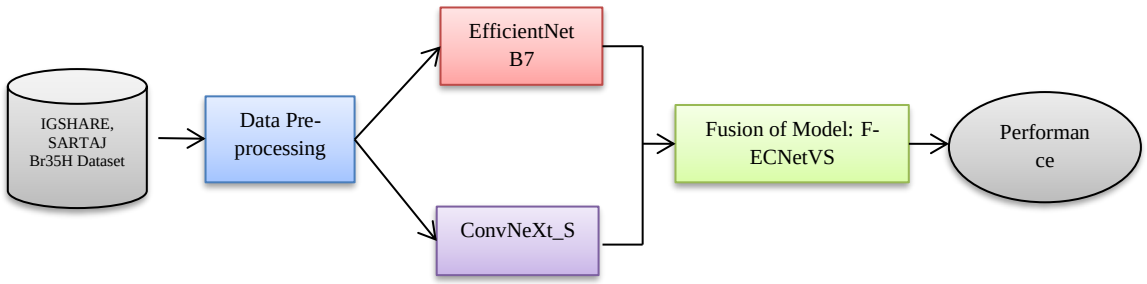

Fig. 11 Dataflow architecture of the proposed F-ECNetVS model

To improve the utilization of complimentary data from both the color and depth maps, the fusion network's objective is to extract color and depth information and integrate them at different spots. The inclusion of the Fusion Module is the primary difference between the color and depth parts and ConvNext [7], which take a similar approach. ConvNext is an upgraded version of ResNet that uses Visual Transformer models' micro and macro design components. ConvNext does substantially better than ResNet, albeit with an identical computing cost. Because of its simplicity, we choose the ConvNext-T variation in this work. Figure 12 (a) shows one such block.

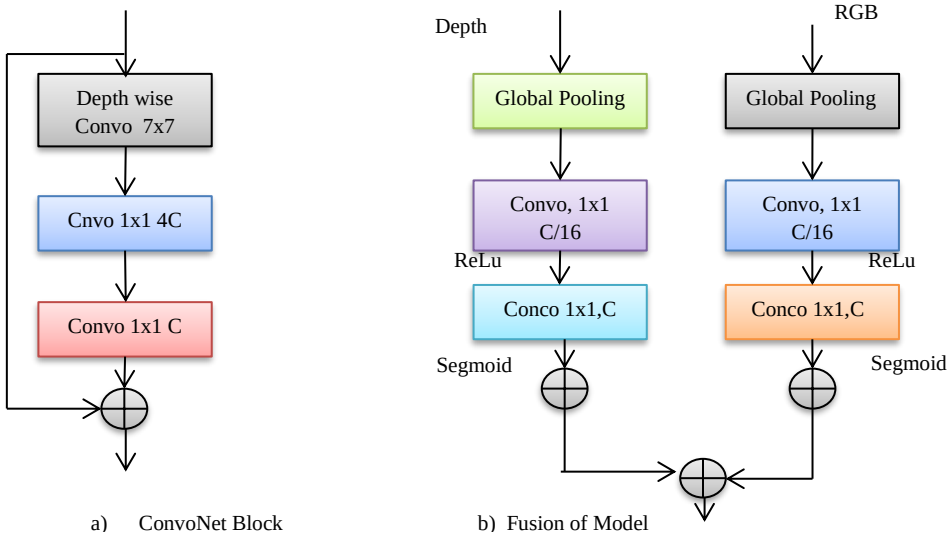

Fig. 12 Block structure a) ConvoNet Block, b) Fusion of Model

Through the Fusion Module, we integrate comprehensive data into the RGB branch at each stage of the core network. This module builds a system that can adapt and learn how to integrate information by utilizing the idea of channel attention, as described in [23]. Figure 13(b) depicts this module's precise configuration. After the features are extracted from the encoder portion, we additionally modify the features with different pooling sizes using the ResNet Module [24]. It is thought that, as previous research has shown, these various

Journal of Information Systems Engineering and Management
2025, 10(46s)
e-ISSN: 2468-4376
https://www.jisem-journal.com/

Research Article

pooling sizes may integrate data from both local and global viewpoints, and have a good impact on segmentation job performance. The Next section covers the result and discussion.

Result and Discussion

4.1 Metrics

Various metrics were employed in the tests to assess the suggested models' performance and compare it with two baseline models: “EfficientNet B7”, and “ConvNeXt_S”. These minimal memory models were compared with models that were put forth. The “F1-score”, “recall”, “accuracy”, and “precision’ were the initial metrics. Our metrics were also extended to multiclass categorization by computing the “macro-average”. Accuracy is the most logical metric to gauge performance since it represents the percentage of correctly identified cases relative to all instances. "TP (true positives)," or cases that were accurately detected as positive, is used to compute this accuracy. To put it simply, accuracy is yes if both the expected and actual classes are yes. True negatives, or TNs for short, are examples of situations when the actual and anticipated class values are both 0 and were accurately classified as negative. When the expected class is yes but the actual class is no, this is known as a false positive, or FP. On the other hand, when the expected class is no but the actual class is yes, this is known as a false negative, or FN. Table 4 represents the evaluation parameters for calculating the model performance.

Table 4: Evaluation parameters.

Metrics Name	Equation	Define
“Precision (P)”	$\frac{TP}{TP + FP}$	The proportion of all expected positive observations to correctly anticipated positive observations.
“Recall (R)”	$\frac{TP}{TP + FN}$	The percentage of real positives that are accurately detected is known as recall.
“F1-score (FS)”	$\frac{2 \times P \times R}{P + R}$	Precision and recall are both taken into consideration by the f1-score.
“Accuracy (A)”	$\frac{TP + TN}{TP + FP + TN + FN}$	The ratio of properly predicted observations to total observations.
“Macro-Average (M-A)”	$\frac{P_1 + P_2 + P_3 + \cdots .. + P_N}{N}$	Is the average precision of every class.

4.2 Performance Evolution of Improved Models

With 196 layers and 54.4 million trainable parameters, the improved version of EfficientNet B7 witnessed an increase in accuracy from the beginning of training to the 40th epoch, reaching 95.98% on both test and training sets. As seen in figure 13, the accuracy trend continued after this, eventually stabilizing at 97.91%

Journal of Information Systems Engineering and Management
2025, 10(46s)
e-ISSN: 2468-4376
https://www.jisem-journal.com/

Research Article

for the training set and 98.27% for the test set. With a high accuracy of 91.68%, the accuracy trend for the EfficientNet B7 training data grew quickly.

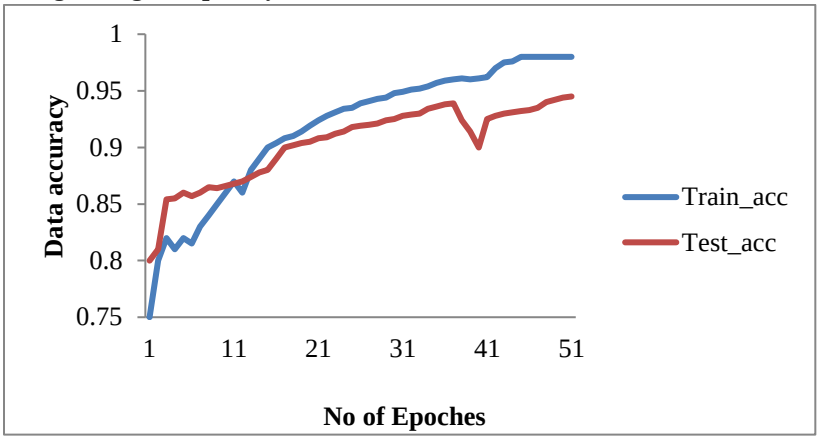

Fig.13 Accuracy curve of EfficientNet B7 model

The model ConvNeXt_S has 149 deep layers with 50.2 million parameters. Between the eleventh and forty-first epochs, the training accuracy reaches a stable phase with a consistency of 95.27%. The accuracy drops after the 40th epoch and settles at 97.23%. As seen in figure 14, the graph rises during the testing phase until the 40th epoch, at which time the precision is recorded at 94.53%.

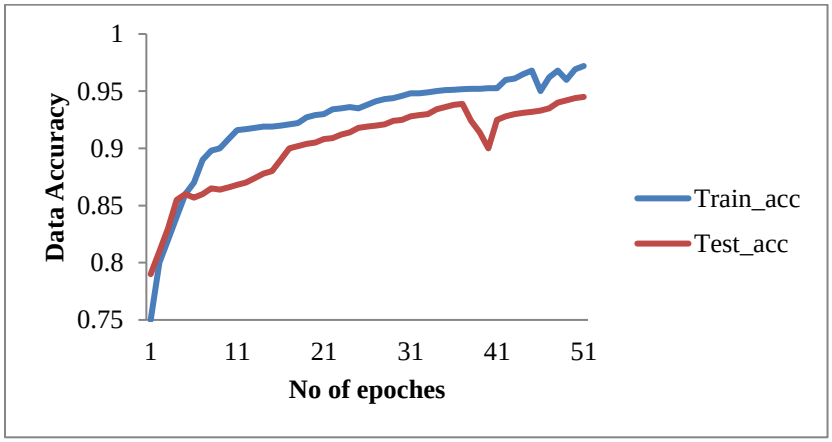

Fig.14 Accuracy curve of ConvNeXt_S model

We calculate the specificity, F1-score, accuracy, and recall rates for every pre-trained model by assessing its efficacy. With an F1-score of 96.58% and an accuracy rate of 98.27%, EfficientNet B7 outperformed other models by a substantial margin. Table 5 shows the performance in terms of different evaluation metrics.

Table 5. Models performance in terms of different evaluation metrics

Model Name	Accuracy (%)	Precision (%)	Sensitivity (%)	Specificity (%)	F1-Score (%)

Journal of Information Systems Engineering and Management
2025, 10(46s)
e-ISSN: 2468-4376
https://www.jisem-journal.com/

Research Article

EfficientNet B7	98.27	95.85	94.18	98.58	96.58
ConvNeXt_S	97.24	93.14	94.23	97.45	91.45
Proposed F-ECNetVS	99.90	94.11	95.18	97.12	97.78

Achieved sensitivity of 94.23% and specificity of 97.45% is the ConvNeXt_S model. Table 6 shows that the EfficientNet B7 model outperforms the other pre-trained models in terms of chest illness prediction. Furthermore, figure 15 shows the EfficientNet B7 model's performance in relation to several assessment measures.

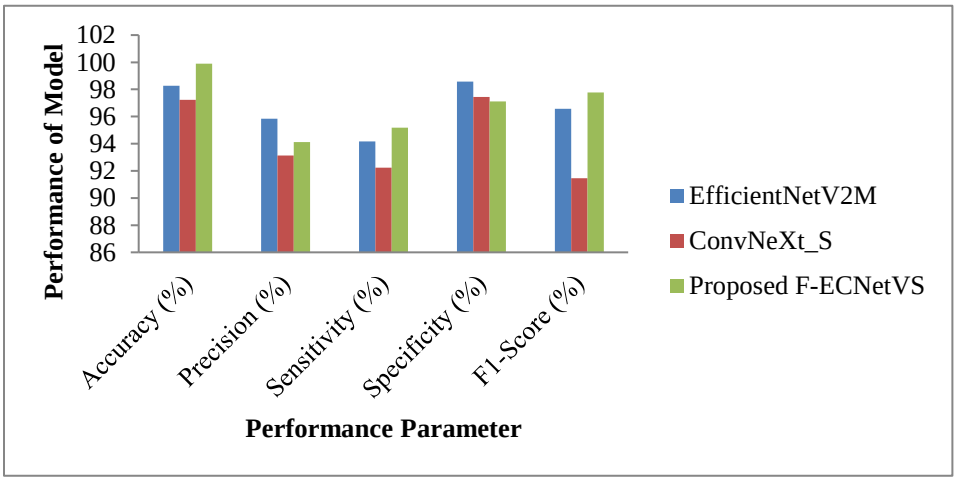

Fig. 15 Models performance in terms of different evaluation terms

More accuracy is shown by the current model EfficientNet B7 than by a number of other pre-trained models. ConvNeXt_S models do not outperform EfficientNet B7 in terms of accuracy when compared. As Figure 15 shows, the performance of various models may be used to explain the little variation in specificity between them. The ensemble learning model using these pre-trained models is shown in the next section, along with all the models arranged in different configurations.

4.3 Ensemble model evaluation performance

This study looks at several ensemble learning models to see if the architecture shown in Figure 15—which makes use of highly-tuned EfficientNet B7 and ConvNeXt_S models—improves their performance. While the ConvNeXt_S model, a two-layer ensemble, shows poorer accuracy, the EfficientNet B7 model performs better than other prototypes that were not trained as well. EfficientNet B7 and ConvNeXt_S models both attain greater accuracy in 79.45 seconds, which is much faster than the rest of the ensemble learning models. As seen in Table 6, the deep ensemble model—which consists of both ConvNeXt_S and EfficientNet B7—achieves more accurate results with three different models in 55.14 seconds. When using these models in a layered strategy, the categorization results are also accurate. With four distinct models combined, the final ensemble model achieves an accuracy of 97.24% and a precision value of 94.87%.

Journal of Information Systems Engineering and Management
2025, 10(46s)
e-ISSN: 2468-4376
https://www.jisem-journal.com/

Research Article

Table 6. Evaluation of different ensemble models

Dataset	Classifier	Precision	Recall	F1-Score	Accuracy
MRI	EfficientNet B7	98.27	95.85	94.18	98.58
	ConvNeXt_S	97.24	93.14	94.23	97.45
	F-ECNetVS	98.90	96.11	96.18	99.88

The performance is evaluated based on different quality assessments. Ensemble learning is being used to demonstrate its effectiveness in comparison to a single model. The value of one parameter named F1-score changes with the change of ensemble models. The ensemble deep learning model as F-ECNetVS shows a 99.88% accuracy value which is far better than another model. The fact that the knowledge acquired by ensembles cannot be understood by the user is a fundamental flaw in existing ensemble methods.

4.3 Discussion

Combination learning models and individual pre-trained models were used in this study to investigate the multiclass classification of high-resolution photos of tomato leaves and choose the best architecture by analyzing various performance-related parameters. In the case of essential FN and FP, the F1 score is applied, while accuracy is used when TP and TN are more relevant. When the distribution of the classes is similar, accuracy can be used, but the F1 score seems an improved statistic in case the distribution of the classes is unbalanced. Figure 16 displays the outcome regarding single and ensemble learning approaches to identify and classify tomato leaf diseases in terms of accuracy and F1 score.

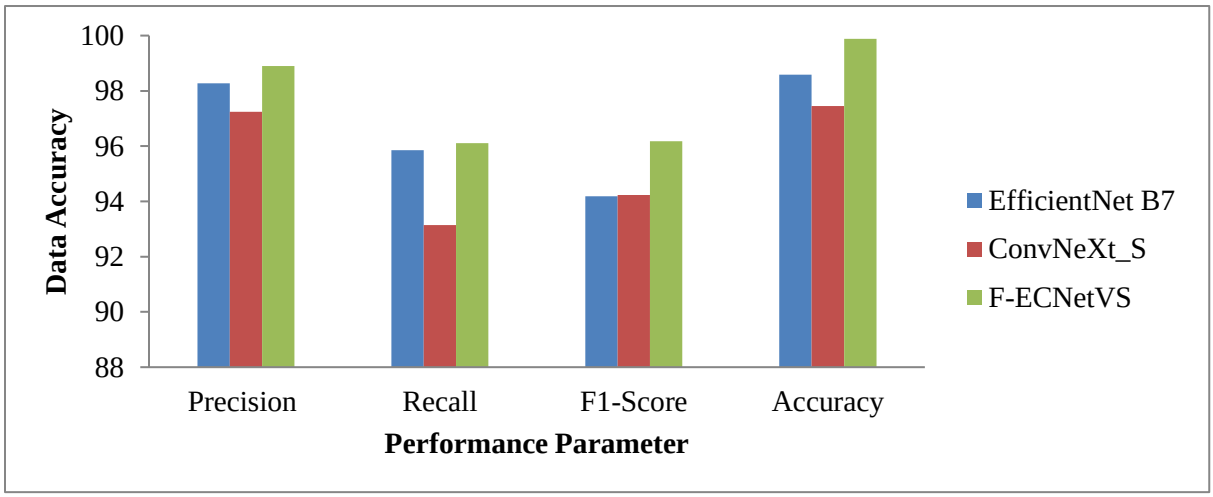

Fig. 16: Single and Ensemble learning models performance

Figure 16 shows a little variance in results between the various deep learning models. In particular, Br35H performs better than other ensemble models such as MRI. Nonetheless, the accuracy of the model appears to be unaffected by the quantity of deep learning components included in the ensemble. In actuality, the outcomes are greatly influenced by the ensemble model selection. In addition, F-ECNetVS took 32,976.83 seconds to train in total, ConvNeXt_S took 41,321.87 seconds, and EfficientNet B7 took 52,481.62 seconds. The time required for both solo and group models to do their tasks is shown in Figure 17.

Journal of Information Systems Engineering and Management
2025, 10(46s)
e-ISSN: 2468-4376
https://www.jisem-journal.com/

Research Article

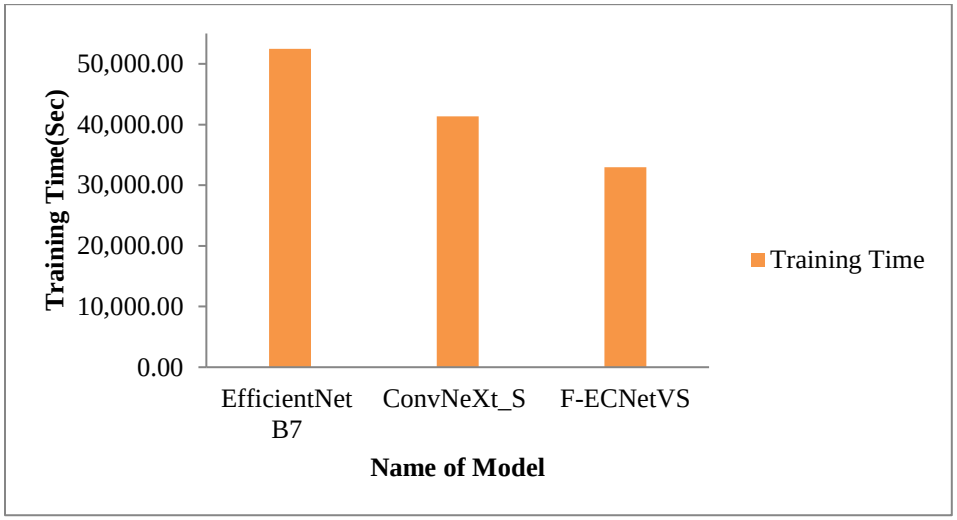

Fig. 17 computation time required by single and ensemble models

Figure 17 shows that although the EfficientNet B7 model produces acceptable results, it is not as fast as it might be because the training procedure takes 52,481.62 seconds. Furthermore, the combined model F-ECNetVS outperforms the ConvNeXt_S model in terms of speed and accuracy rate on Precession, with a rate of 98.90%.

5. Conclusion

The following study classifies tomato leaf disease using different ten classes of super-resolution images which are: Glioma, Meningioma, Pituitary, and Notumor. using both ensemble and single learning models (EfficientNet B7, ConvNeXt_S). The pre-trained model EfficientNet B7 shows an attained 98.27% accuracy as well as shows 96.58 % F1-score which is far better than other models. The F-ECNetVS exhibits enhanced precision in identifying and categorizing data for a duration of 32,976.83 seconds, with a 99.88% accuracy rate, in addition to a sophisticated deep learning model. The created F-ECNetVS model has been used to diagnose brain cancers among other medical issues. Furthermore, there is no evidence to support the claim that greatly improving an ensemble's accuracy of numerous deep-learning models increases the model's accuracy. A new study aims to develop a comprehensive system for brain tumor illness identification by combining deep learning and other methods including form, color, and texture analysis with feature extraction techniques. Increasing the diversity of datasets, experimenting with more complex feature extraction approaches, and utilizing alternative information combining methodologies are all potential avenues to enhance the model's performance.

Acknowledgement.

I would like to give my sincere thanks to Dr.S.P.Singh, Associate Professor, Department of Computer Science & Engineering, Rashtrakavi Ramdhari Singh Dinkar College of Engineering, Begusarai-851134 for his valuable suggestion for analyzing the data.

Competing Interest

The Authors declare that they have no known competing financial interests or personal relationships that could have appeared to influence the work reported in this paper.

Ethics Declarations

The authors declare that they have no conflict of interest

Data Availability

The authors are ready to provide data on request.

REFERENCES

[1] Mehrotra R, Ansari MA, Agrawal R, Anand RS (2020) A transfer learning approach for AI-based classification of brain tumors. Machine Learning with Applications. 2:100003.

[2] Haque R, Hassan MM, Bairagi AK, Shariful Islam SM. NeuroNet19 (2024): an explainable deep neural network model for the classification of brain tumors using magnetic resonance imaging data. Scientific Reports. 14(1):1524.

[3] Attallah O, Sharkas MA, Gadelkarim H (2020) Deep Learning Techniques for Automatic Detection of Embryonic Neurodevelopmental Disorders. Diagnostics, 10, 27.

[4] Stadlbauer A, Marhold F, Oberndorfer S, Heinz G, Buchfelder M, Kinfe TM, Meyer-Bäse A (2022) Radiophysiomics: brain tumors classification by machine learning and physiological MRI data. Cancers. 14(10):2363.

[5] Haq AU, Li JP, Kumar R, Ali Z, Khan I, Uddin MI, Agbley BL.(2023) MCNN: a multi-level CNN model for the classification of brain tumors in IoT-healthcare system. Journal of Ambient Intelligence and Humanized Computing. 14(5):4695-706.

[6] Tandel GS, Tiwari A, Kakde OG, Gupta N, Saba L, Suri JS (2023). Role of ensemble deep learning for brain tumor classification in multiple magnetic resonance imaging sequence data. Diagnostics. 13(3):481.

[7] Saboor A, Li JP, Ul Haq A, Shehzad U, Khan S, Aotaibi RM, Alajlan SA. (2024) DDFC: deep learning approach for deep feature extraction and classification of brain tumors using magnetic resonance imaging in E-healthcare system. Scientific Reports. 14(1):6425.

[8] Gumaei A, Hassan MM, Hassan MR, Alelaiwi A, Fortino G.(2019) A hybrid feature extraction method with regularized extreme learning machine for brain tumor classification. IEEE Access.,7:36266-73.

[9] Hussain UN, Khan MA, Lali IU, Javed K, Ashraf I, Tariq J, Ali H, Din A.(2020) A unified design of ACO and skewness based brain tumor segmentation and classification from MRI scans. Journal of Control Engineering and Applied Informatics.22(2):43-55.

[10] Khan MA, Ashraf I, Alhaisoni M, Damaševičius R, Scherer R, Rehman A, Bukhari SA (2020). Multimodal brain tumor classification using deep learning and robust feature selection: A machine learning application for radiologists. Diagnostics. 10(8):565.

[11] Younis A, Qiang L, Nyatega CO, Adamu MJ, Kawuwa HB.(2022) Brain tumor analysis using deep learning and VGG-16 ensembling learning approaches. Applied Sciences. ,12(14):7282.

[12] Kaur P, Harnal S, Tiwari R, Alharithi FS, Almulihi AH, Noya ID, Goyal N.(2021) A hybrid convolutional neural network model for diagnosis of COVID-19 using chest X-ray images. International Journal of Environmental Research and Public Health. 18(22):12191.

[13] Hashemzehi R, Mahdavi SJ, Kheirabadi M, Kamel SR. Detection of brain tumors from MRI images base on deep learning using hybrid model CNN and NADE. Biocybern Biomed Eng 40 (3): 1225–1232.

[14] Díaz-Pernas FJ, Martínez-Zarzuela M, Antón-Rodríguez M, González-Ortega D (2021). A deep learning approach for brain tumor classification and segmentation using a multiscale convolutional neural network. InHealthcare (Vol. 9, No. 2, p. 153). MDPI.
[15] Kokkalla S, Kakarla J, Venkateswarlu IB, Singh M(2021). Three-class brain tumor classification using deep dense inception residual network. Soft Computing. 25(13):8721-9.
[16] Saeedi S, Rezayi S, Keshavarz H, R. Niakan Kalhori S (2023). MRI-based brain tumor detection using convolutional deep learning methods and chosen machine learning techniques. BMC Medical Informatics and Decision Making. 23(1):16.
[17] Budati AK, Katta RB (2022). An automated brain tumor detection and classification from MRI images using machine learning technique s with IoT. Environment, Development and Sustainability.24(9):10570-84.
[18] Mahmud MI, Mamun M, Abdelgawad A (2023) A deep analysis of brain tumor detection from mr images using deep learning networks. Algorithms. 16(4):176.
[19] Nassar SE, Yasser I, Amer HM, Mohamed MA (2024). A robust MRI-based brain tumor classification via a hybrid deep learning technique. The Journal of Supercomputing. 80(2):2403-27.
[20] Talukder MA, Islam MM, Uddin MA, Akhter A, Pramanik MA, Aryal S, Almoyad MA, Hasan KF, Moni MA (2023). An efficient deep learning model to categorize brain tumor using reconstruction and fine-tuning. Expert systems with applications. 230:120534.
[21] Zulfiqar F, Bajwa UI, Mehmood Y (2023). Multi-class classification of brain tumor types from MR images using EfficientNets. Biomedical Signal Processing and Control. 84:104777.
[22] Yousaf F, Iqbal S, Fatima N, Kousar T, Rahim MS. Multi-class disease detection using deep learning and human brain medical imaging. Biomedical Signal Processing and Control. 2023 Aug 1;85:104875.
[23] Raza A, Ayub H, Khan JA, Ahmad I, S. Salama A, Daradkeh YI, Javeed D, Ur Rehman A, Hamam H (2022). A hybrid deep learning-based approach for brain tumor classification. Electronics. 11(7):1146.
[24] Bhanothu Y, Kamalakannan A, Rajamanickam G (2020) Detection and classification of brain tumor in MRI images using deep convolutional network. In2020 6th international conference on advanced computing and communication systems (ICACCS) (pp. 248-252). IEEE.
[25] Saba T, Mohamed AS, El-Affendi M, Amin J, Sharif M (2020). Brain tumor detection using fusion of hand crafted and deep learning features. Cognitive Systems Research. 59:221-30.
[26] Sadad T, Rehman A, Munir A, Saba T, Tariq U, Ayesha N, Abbasi R (2021). Brain tumor detection and multi-classification using advanced deep learning techniques. Microscopy Research and Technique. 84(6):1296-308.
[27] Li, D., De, L., Keqing, L. et al (2023). Extreme Learning Machine (ELM) Method for Classification of Preschool Children Brain Imaging. J Autism Dev Disord.
[28] Asiri AA, Shaf A, Ali T, Aamir M, Usman A, Irfan M, Alshamrani HA, Mehdar KM, Alshehri OM, Alqhtani SM. (2023) Multi-Level Deep Generative Adversarial Networks for Brain Tumor Classification on Magnetic Resonance Images. Intelligent Automation & Soft Computing.Apr 1;36(1).
[29] Deepak S, Ameer PM (2023) Brain tumor categorization from imbalanced MRI dataset using weighted loss and deep feature fusion. Neurocomputing. 520:94-102.
[30] Sayedgomaa. Brain Tumor Kaggle. Available online: https://www.kaggle.com/code/sayedgomaa/brain-tumor/notebook (accessed on 21 June 2024).
[31] Rasheed Z, Ma YK, Ullah I, Al Shloul T, Tufail AB, Ghadi YY, Khan MZ, Mohamed HG (2023). Automated classification of brain tumors from magnetic resonance imaging using deep learning. Brain Sciences.13(4):602.
[32] Ozkaraca O, Bagrıacık OI, Guruler H, Khan F, Hussain J, Khan J, Laila UE (2023). Multiple brain tumor classification with dense CNN architecture using brain MRI images. Life. 13(2):349.

[33] Sharif MI, Li JP, Khan MA, Kadry S, Tariq U.(2024) M3BTCNet: multi-model brain tumor classification using metaheuristic deep neural network features optimization. Neural Computing and Applications. 36(1):95-110.

[34] Özyurt F, Sert E, Avcı D.(2020) An expert system for brain tumor detection: Fuzzy C-means with super-resolution and convolutional neural network with extreme learning machine. Medical Hypotheses.134:109433.

[35] Wang S, Du S, Atangana A, Liu A, Lu Z (2018). Application of stationary wavelet entropy in pathological brain detection. Multimedia tools and applications.77:3701-14.

[36] Attique Khan M, Sharif M, Akram T, Kadry S, Hsu CH (2022). A two-stream deep neural network-based intelligent system for complex skin cancer types classification. International Journal of Intelligent Systems. 37(12):10621-49.

[37] Aziz A, Attique M, Tariq U, Nam Y, Nazir M, Jeong CW, Mostafa RR, Sakr RH (2021). An Ensemble of Optimal Deep Learning Features for Brain Tumor Classification. Computers, Materials & Continua. 69(2).

[38] Wang SH, Phillips P, Sui Y, Liu B, Yang M, Cheng H.(2018) Classification of Alzheimer's disease based on an eight-layer convolutional neural network with leaky rectified linear unit and max pooling. Journal of medical systems.42:1-1.

[39] Khairandish MO, Sharma M, Jain V, Chatterjee JM, Jhanjhi NZ (2022). A hybrid CNN-SVM threshold segmentation approach for tumor detection and classification of MRI brain images. Irbm. 43(4):290-9.

[40] Hu K, Gan Q, Zhang Y, Deng S, Xiao F, Huang W, Cao C, Gao X.(2019) Brain tumor segmentation using multi-cascaded convolutional neural networks and conditional random field. IEEE Access.7:92615-29.